


ORIGINAL ARTICLE

Open Access



# Fabrication of Superhydrophobic Micro Post Array on Aluminum Substrates Using Mask Electrochemical Machining

Jing Sun<sup>1,2</sup>, Wei Cheng<sup>1,2</sup>, Jin-Long Song<sup>1,2\*</sup> , Yao Lu<sup>3</sup>, Yan-Kui Sun<sup>1</sup>, Liu Huang<sup>1</sup>, Xin Liu<sup>1</sup>, Zhu-Ji Jin<sup>1</sup>, Claire J. Carmalt<sup>3</sup> and Ivan P. Parkin<sup>3</sup>

## Abstract

Surfaces with controllable micro structures are significant in fundamental development of superhydrophobicity. However, preparation of superhydrophobic surfaces with array structures on metal substrates is not effective using existing methods. A new method was presented to fabricate super-hydrophobic post arrays on aluminum (Al) substrates using mask electrochemical machining and fluoridation. Electrochemical etching was first applied on Al plates with pre-prepared photoresist arrays to make the post array structures. Surface modification was subsequently applied to reduce the surface energy, followed by interaction with water to realize superhydrophobicity. Simulation and experimental verification were conducted to investigate how machining parameters affect the array structures. Analysis of the water contact angle was implemented to explore the relationship between wettability and micro structures. The results indicate that superhydrophobic surfaces with controllable post structures can be fabricated through this proposed method, producing surfaces with high water static contact angles.

**Keywords:** Superhydrophobicity, Aluminum substrates, Mask electrochemical machining, Micro post arrays

## 1 Introduction

Superhydrophobic surfaces have become a research focus owing to their various applications in self-cleaning [1, 2], corrosion resistance [3, 4] and anti-icing [5]. It has been proven both surface energy [6] and roughness [7, 8] are the crucial factors to obtain superhydrophobicity. Based on these two factors, coating [9, 10], chemical depositing [11] and many other approaches have been advanced to prepare artificial superhydrophobic surfaces. On account that the surface modification technics to lower surface energy are well-developed, method to construct the rough structures becomes a key issue. There are two forms of rough surfaces that can be applied to obtain superhydrophobicity, surfaces with disordered structures and ordered structures. The ordered structured arrays

with designed parameters appear to be more effective in revealing the mechanism of superhydrophobic surfaces or endowing special functions [12, 13]. For example, it has been reported recently that micro arrays with specific parameters allow a reduction in contact time when water droplets impact on this kind of superhydrophobic surfaces [14, 15], which results in these surfaces with micro post arrays being promising for application prospects in anti-icing from freezing rain. Several methods to prepare superhydrophobic post arrays have been reported, including photolithography, electric spark wire cutting and laser texturing. Öner and co-workers [16] obtained superhydrophobic post arrays on silicon substrates with a variety of topographies by changing the photomasks in lithography process. Butt et al. [17] used lithography to prepare SU-8 photoresist arrays with superhydrophobicity. Liu et al. [14] prepared superhydrophobic tapered posts on copper (Cu) substrates by using wire electro discharge machining followed by chemical etching and coating thin polymer. Van et al. [18] utilized laser texturing as well as surface energy modification to fabricate

\*Correspondence: songjinlong@dlut.edu.cn

<sup>1</sup> Key Laboratory for Precision and Non-traditional Machining Technology of the Ministry of Education, Dalian University of Technology, Dalian 116024, China

Full list of author information is available at the end of the article

superhydrophobic square posts on stainless steel substrates. However, for the aforementioned methods, the machining efficiency of wire electro discharge machining for large-area array structures is very low, in addition, it is very difficult to fabricate post arrays with diameters of several tens of micrometers. Laser texturing not only requires expensive equipment but also is difficult to efficiently fabricate post arrays with diameter of several tens of micrometers. Photolithography is a highly efficient method to prepare superhydrophobic micro arrays, but currently, it can only be applied on silicon and photoresist substrates. Considering that metals are one of the most widely used materials, an effective method to fabricate superhydrophobic array structures on engineering metals has great significance for moving superhydrophobic surfaces towards real-world applications.

Mask electrochemical machining (MECM), which combines photolithography and micro electrochemical machining, is widely used to prepare micro-pits arrays on engineering metal materials because of its low cost, easy operation process and high machining efficiency [19–22]. Here, we extended this technique into the area of fabricating superhydrophobic post arrays on aluminum (Al) substrates. The influence of machining parameters on the array structures was investigated by simulation and then verified by experiment. Based on the fabricated post array structures, the relationship between wettability and microstructural parameters was further studied.

## 2 Experiment

The preparation process of the superhydrophobic post arrays is shown in Figure 1. Al plate (35 mm × 35 mm × 2 mm, Dalian Al material manufacturer, China) was first polished by abrasive paper to remove surface oxide and then cleaned in an ultrasonic bath. After drying, a thin film of positive photoresist (BP212-37S, Beijing Kehua Microelectronics, China) of 1.5 μm thickness was spun on the surface with rotation speed 450 r/min for 15 s and 2000 r/min for 45 s. Then the obtained plate was prebaked at 85 °C for 45 min and

subsequently exposed to a UV light source for 20 s. After that, the plate was developed in 0.5 wt.% aqueous NaOH solution for 4 min. Then, after being postbaked at 85 °C for 45 min, the Al plate with the photoresist array was prepared.

The as-prepared Al plate and Cu plate of the same size were placed face to face with a separation distance of 10 mm in the electrolyte tank. Then the Al plate was electrochemically machined as a positive electrode under ultrasonic vibration in 15.0 wt.% aqueous NaNO<sub>3</sub> solution to generate the designed array structures. And the current load was applied by a DC electrical source which exports current constantly and can provide voltage up to 60 V. After that, the fabricated plate was ultrasonically cleaned and then immersed in 1.0 wt.% fluoroalkylsilane–ethanol solution for 2 h at room temperature (25 °C) to lower its surface energy.

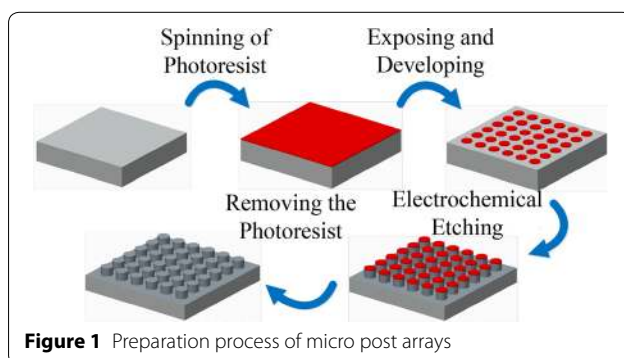
Micro morphologies of the samples were observed via scanning electron microscope (SEM, JSM-6360LV, Japan) and surface profiler (XZ-230, Zygo, America). Static contact angle (CA) measurements were performed by optical contact angle meter (DSA100, Krüss, Germany) at room temperature.

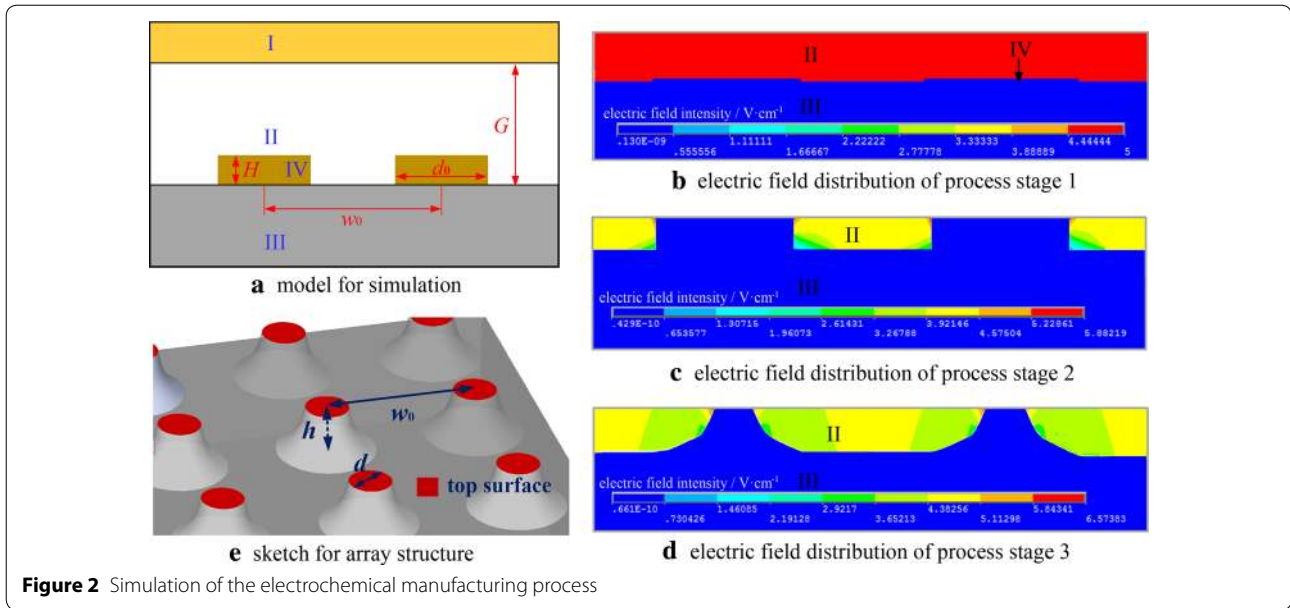
## 3 Results and Discussions

### 3.1 Modeling and Analyzing of MECM Fabrications of Micro Post Arrays

In order to obtain micro post arrays with the required structures, a 2D model as shown in Figure 2(a) was built in the ANSYS platform to study the variation of the array structures on process time ( $t$ ) and current density ( $I$ ). Domains I~IV in the figure represent the Cu electrode, electrolyte, Al plate and photoresist, respectively. The distance between positive and negative electrode ( $G$ ) and the thickness of the photoresist film ( $H$ ) were set to 10 mm and 1.5 μm, respectively. The photoresist parameters  $d_0=150$  μm,  $w_0=250$  μm were set in accordance with the photomask we used.

Figure 2(b)–(d) show the electric field intensity nephograms of different stages in the MECM process (these images were vertically enlarged to enable better imaging). At the beginning, the electric field was distributed homogeneously (Figure 2(b)) because comparing with  $G$ ,  $H$  was so small that the photoresists had nearly no influence on the electric field distribution. After the removal of some of the Al plate, the structural changes led to a re-distribution of the electric field, and every surface that was exposed to the electrolyte had an electric load on it (Figure 2(c)). As a result, the sidewalls of the micro structures started to be corroded. And the structures of the micro array changed both vertically and horizontally over time. Eventually, the micro posts changed to truncated cones as shown in Figure 2(d). According to that, a 3D





structural model was sketched and shown in Figure 2(e). The diameter of the top surface of the post ( $d$ ) and post height ( $h$ ) were utilized as the critical parameters to describe the post array structures.

During the manufacturing process, ranges of domain II (electrolyte) and domain III (Al plate) changed continuously because of Al material removal. The varying velocity of the electrolyte-Al plate contact line ( $V$ ) obeyed Faraday's law,

$$V = \eta\omega\kappa E, \tag{1}$$

where  $\eta$  refers to the current efficiency,  $\omega$  denotes the electrochemical equivalent of Al material,  $\kappa$  represents the electric conductivity of 15.0 wt.% aqueous  $\text{NaNO}_3$  solution,  $E$  is electric field intensity of nodes and it can be solved by simulation.

For an arbitrary node  $M_n(x_n, y_n)$  on the contact line of electrolyte and Al plate, the coordinate of corresponding new node  $M_{n+1}(x_{n+1}, y_{n+1})$  after a time interval  $\Delta t$  could be calculated as follows:

$$x_{n+1} = x_n + \eta\omega\kappa E_X \Delta t, \tag{2}$$

$$y_{n+1} = y_n + \eta\omega\kappa E_Y \Delta t, \tag{3}$$

where  $E_X$  and  $E_Y$  are the components of  $E$  along  $X$  axis and  $Y$  axis, respectively.

New boundaries of domain II and domain III were generated by connecting all the nodes computed. These boundaries were used to set up a new model from which subsequent model boundary variations could be obtained. Therefore, an iterative method to set up time series model that represents the structural geography was

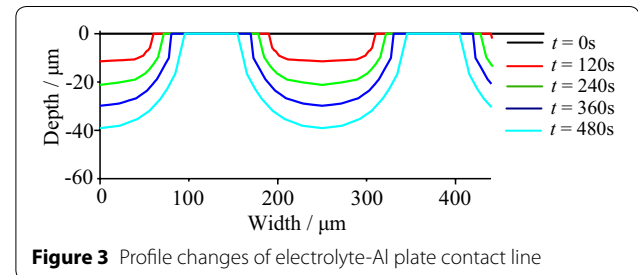
given. After several times of iterative calculations, correlation between  $t$  and the micro structures was revealed. The variation of electrolyte-Al plate contact line with  $t$  without considering of  $\eta$  when a  $0.6 \text{ A/cm}^2$  current load was applied is shown in Figure 3.

In the iterative calculation, variations of the node coordinates were proportional to the effective current density  $\eta I$  and the process time  $t$ . And the result of simulation indicated that a uniform structure could be obtained when we adjusted  $I$  and  $t$  to make  $\eta It$  equal. So we established  $\eta It$  as the independent variable, after considering the changes of  $I$  with the range changes of the processing area in a constant current mode, a polynomial fitting was carried out to establish the variation laws of  $d$  and  $h$ , which could be deduced as follows:

$$d = d_0 - 0.563\eta It + 2.77e^{-4}(\eta It)^2, \tag{4}$$

$$h = 0.298\eta It - 4.32e^{-4}(\eta It)^2. \tag{5}$$

Moreover, although the 15.0 wt.% aqueous  $\text{NaNO}_3$  solution used in this experiment as electrolyte had a current efficiency that increased non-linearly with the



growth of current density. Under our processing condition, we noticed that  $\eta$  is approximately 47.5% when the electric current density was constant 3–7 A/cm<sup>2</sup>. So in the subsequent manufacturing, the current density was chose within the range of 3–7 A/cm<sup>2</sup>, and the variation laws of  $d$  and  $h$  with  $I$  and  $t$  could be expressed as follows:

$$d = d_0 - 0.267It + 6.25e^{-5}(It)^2, \tag{6}$$

$$h = 0.142It - 9.75e^{-5}(It)^2. \tag{7}$$

And these variation laws are illustrated in Figure 4.

### 3.2 Comparison of Simulation and Fabricated Results of the Micro Post Arrays

A comparison of fabricated Al plates and simulant results was performed to verify the accuracy of the above simulation. Figure 5 shows the section profiles of micro arrays produced under current density of 4 A/cm<sup>2</sup> for 90 s and 6 A/cm<sup>2</sup> for 60 s, as well as simulant result when  $It = 360 \text{ As/cm}^2$ .

Shown in Figure 6(a), (b) are the experimental verification at various time points of  $d$  and  $h$ , respectively, when  $I = 6 \text{ A/cm}^2$ .

It can be observed from Figure 5 that there was only a difference in the sidewall profiles among the three lines.

Because current density was reckoned as a constant in the simulation, for areas of low electric intensity in Figure 2(c), (d), current efficiency  $\eta$  was applied inaccurately owing to the non-linear property of electrolyte. Therefore, a deviation of sidewall profile occurred consequently because these low intensity areas were always at the bottom and sidewalls of the posts.

But for the top surface and the areas far from the post centers, electric intensities tended to be close to the loads

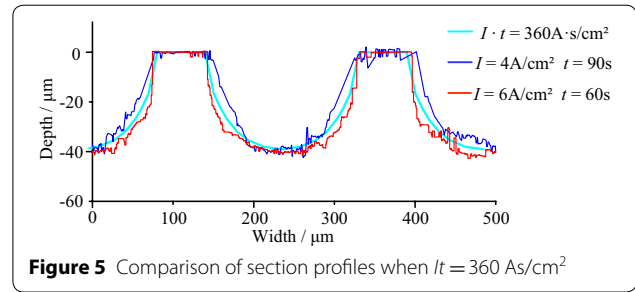


Figure 5 Comparison of section profiles when  $It = 360 \text{ As/cm}^2$

applied, so  $\eta$  was used correctly, and the key parameters  $d$  and  $h$  were predicted precisely as shown in Figure 6. Thus,  $d$  and  $h$  of the post arrays can be accurately controlled by adjusting  $I$  and  $t$  according to Eqs. (6), (7).

Shown in Figure 7 are SEM images of the fabricated Al plate with expected  $d$  and  $h$  when  $I = 6 \text{ A/cm}^2$  and  $t = 100 \text{ s}$ , the anticipative micro post arrays were obtained on Al substrates.

### 3.3 Analysis of Wettability of the Post Arrays

According to the observation of solid-liquid contact interfaces on as-prepared Al plates, two typical modes shown in Figure 8(a) were observed. These two modes were in accordance with the Cassie–Baxter model [8] and Wenzel model [9] as shown in Figure 8(b), respectively.

And after further measuring of static water CAs of fabricated Al plates, we found that the superhydrophobic surfaces where the CA was larger than 150° were in the contact mode of Cassie while the non-superhydrophobic surfaces were not. So static CAs of fabricated superhydrophobic surfaces can be explained by Cassie equation [8] as follows:

$$\cos\theta^* = \varphi_s (\cos\theta_0 + 1) - 1, \tag{8}$$

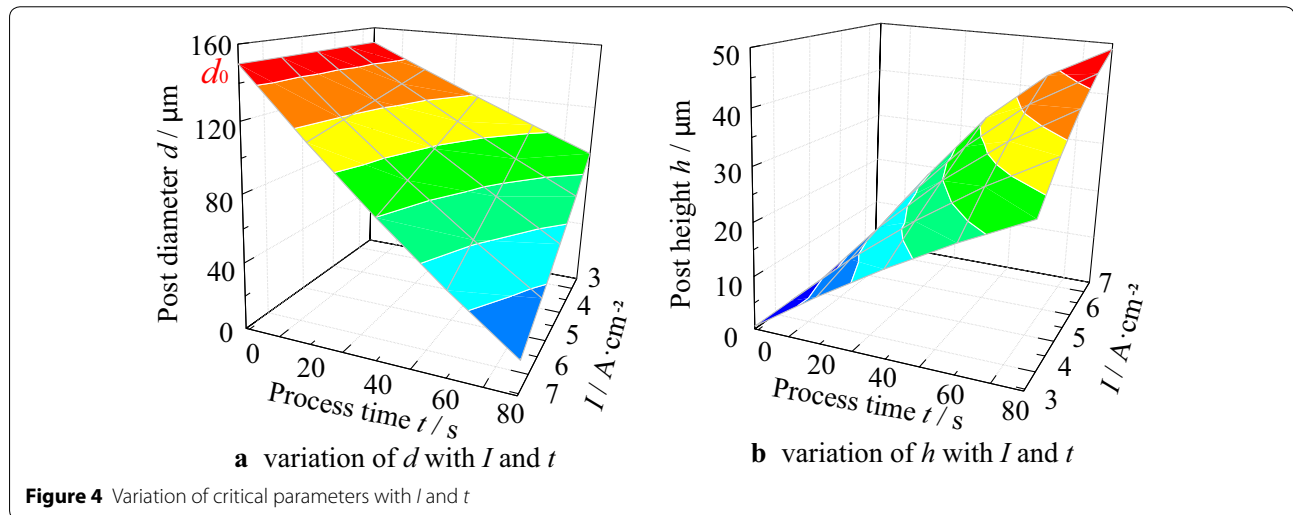
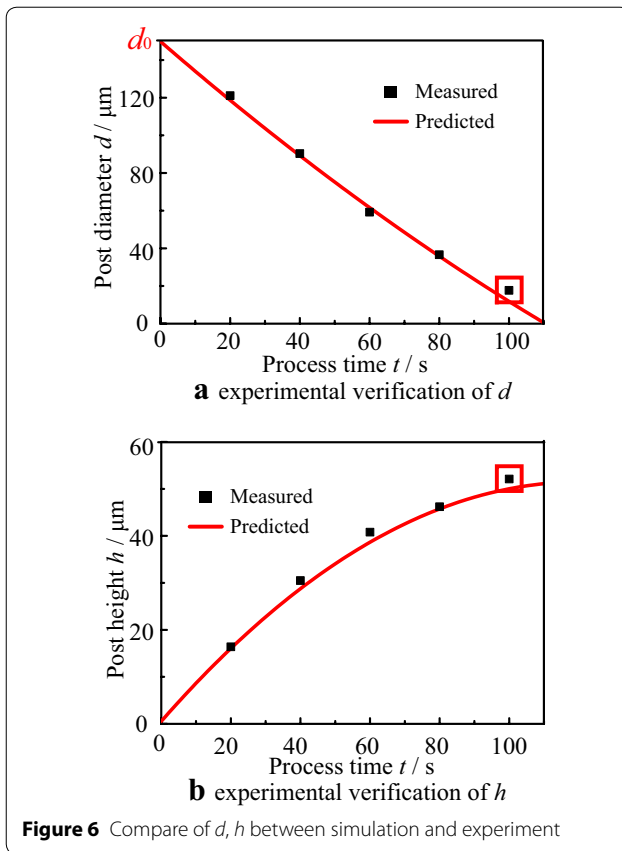
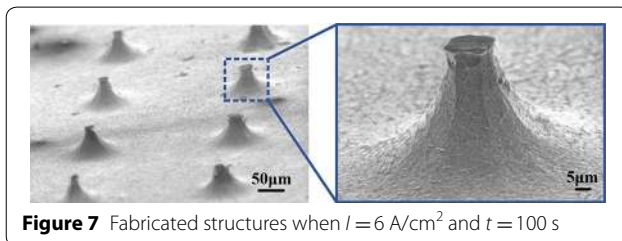


Figure 4 Variation of critical parameters with  $I$  and  $t$



**Figure 6** Compare of  $d$ ,  $h$  between simulation and experiment



**Figure 7** Fabricated structures when  $I = 6 \text{ A/cm}^2$  and  $t = 100 \text{ s}$

where  $\theta^*$  is the theoretical CA of Cassie model,  $\theta_0$  denotes the instinct CA of Al after modification,  $\varphi_s$  refers to the fraction of solid-liquid interface in the composite interface.

Apparent CAs ( $\theta_A$ ) of Al plates of different post height and solid fraction were compared with  $\theta^*$  and shown in Figure 9. These Al plates were fabricated by MECM with different photomasks that had a diverse center-to-center distance  $w_0$  in the range of 160–200  $\mu\text{m}$ . And according to the Cassie theory, Al plates with different  $d$  and  $w_0$  would have the same CA if they had the same solid fraction  $\varphi_s$ .

The reason that structures positioned in the gray area of Figure 9 don't show superhydrophobicity can be explained as follows:

- (1) For a post array with certain diameter, the post height has to exceed a threshold to prevent the water droplet from collapsing into the microstructures [23–25]. Arrays of 20  $\mu\text{m}$  post height were non-superhydrophobic as they failed to suspend the water droplet on the posts as depicted in the Cassie model.
- (2) The capillary pressure  $P_c$  of a fabricated micro array can be calculated as follows [26]:

$$P_c = -\frac{4d}{w_0^2}\gamma \cos\theta_0, \quad (9)$$

where  $\gamma$  refers to the surface tension coefficient of water. When  $\varphi_s$  was extremely small, capillary pressure provided by the micro array was low and the water droplet could not be suspended either. Therefore, if the center-to-center distance  $w_0$  is much larger than  $d$ , these arrays were not superhydrophobic regardless of the post height.

- (3) When the value of  $\varphi_s$  was large enough, the micro arrays were not superhydrophobic according to Eq. (8). A difference in the contact mode, as shown in Figure 8 resulted in a deviation between apparent CAs and theoretical CAs in this experiment.

For superhydrophobic surfaces shown in the golden area of Figure 9,  $\theta_A$  could be accurately predicted because they matched well with  $\theta^*$ . For a micro cylindrical array, the solid fraction can be deduced as follows:

$$\varphi_s = \frac{\pi d^2}{4w_0^2} \quad (10)$$

Combining Eq. (10) with Eq. (8), the correlation between  $\theta_A$  and microstructure of the micro post array can be given as,

$$\cos\theta_A = \frac{\pi d^2}{4w_0^2}(\cos\theta_0 + 1) - 1 \quad (11)$$

Thus, according to Eqs. (6) and (11), microstructures as well as apparent CAs of the superhydrophobic post arrays can be precisely controlled by adjusting  $I$  and  $t$  in the MECM process.

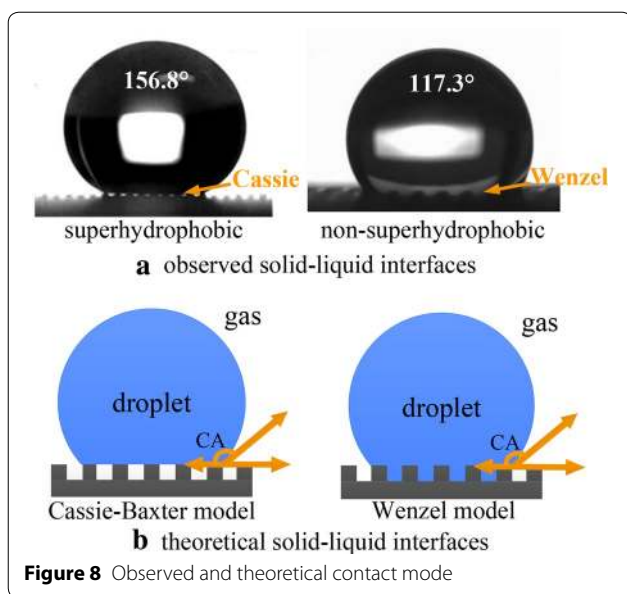


**Figure 8** Observed and theoretical contact mode

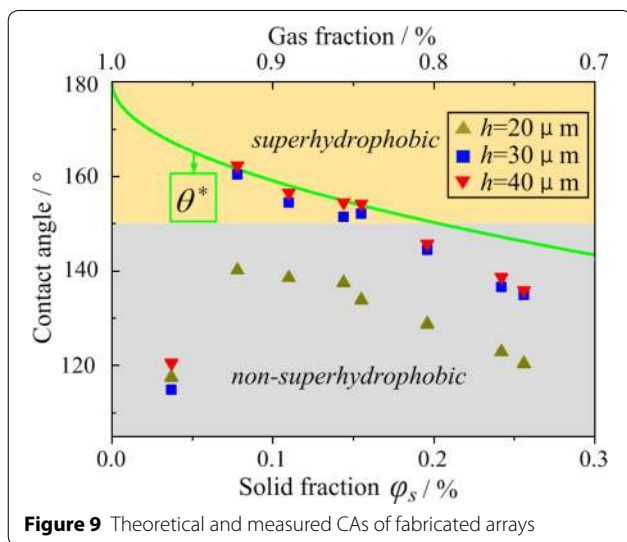


**Figure 9** Theoretical and measured CAs of fabricated arrays

#### 4 Conclusions

- (1) A facile method, combining photolithography, electrochemical machining with surface energy modification, was developed to fabricate superhydrophobic micro post arrays on aluminum substrates.
- (2) According to the simulant and experimental results, after a center-to-center distance is determined, the key structural parameters  $d$  and  $h$  of the post arrays can be precisely controlled by adjusting  $I$  and  $t$  in the MECM.
- (3) The correlation of array structure and apparent water contact angle for Al plates fabricated through the proposed method coincided with the Cassie-

Baxter model. Thus, the structures and water CAs of superhydrophobic micro post arrays fabricated through this method are both controllable.

#### Authors' Contributions

J-LS and JS were in charge of the whole trial; WC wrote the manuscript; YL, Y-KS and LH assisted with sampling and laboratory analyses. All authors read and approved the final manuscript.

#### Author details

<sup>1</sup> Key Laboratory for Precision and Non-traditional Machining Technology of the Ministry of Education, Dalian University of Technology, Dalian 116024, China. <sup>2</sup> Collaborative Innovation Center of Major Machine Manufacturing in Liaoning, Dalian University of Technology, Dalian 116024, China. <sup>3</sup> Department of Chemistry, University College London, 20 Gordon Street, London WC1H 0AJ, UK.

#### Authors' Information

Jing Sun, born in 1974, is currently an associate professor at Key Laboratory for Precision and Non-traditional Machining Technology of the Ministry of Education and Collaborative Innovation Center of Major Machine Manufacturing in Liaoning, Dalian University of Technology, China. She received her PhD degree from Dalian University of Technology, China, in 2009. Her research interests include non-traditional machining.

Wei Cheng, born in 1993, is currently a master candidate at Key Laboratory for Precision and Non-traditional Machining Technology of the Ministry of Education and Collaborative Innovation Center of Major Machine Manufacturing in Liaoning, Dalian University of Technology, China.

Jin-Long Song, born in 1987, is currently an associate professor at Key Laboratory for Precision and Non-traditional Machining Technology of the Ministry of Education and Collaborative Innovation Center of Major Machine Manufacturing in Liaoning, Dalian University of Technology, China. He received his PhD degree under Prof. Wenji Xu from Dalian University of Technology, China. During his PhD, he studied in Department of Mechanical and Industrial Engineering, University of Illinois at Chicago, USA for 1 year as a joint PhD student under the supervision of Prof. Constantine M. Megaridis. After obtained PhD degree, he worked at Center of Smart Interfaces, TU Darmstadt as an Alexander von Humboldt (AvH) Fellow under the supervision of Prof. Steffen Hardt. His research interests involve non-traditional machining, micro electrochemical machining, surface engineering, and wettability.

Yao Lu, born in 1986, is currently a postdoctor at Department of Mechanical Engineering, University College London, UK. He received his PhD degree from University College London, UK, in 2017.

Yan-Kui Sun, born in 1990, is currently a PhD candidate at Key Laboratory for Precision and Non-traditional Machining Technology of the Ministry of Education, Dalian University of Technology, China.

Liu Huang, born in 1990, is currently a master candidate at Key Laboratory for Precision and Non-traditional Machining Technology of the Ministry of Education, Dalian University of Technology, China.

Xin Liu, born in 1981, is currently an associate professor at Key Laboratory for Precision and Non-traditional Machining Technology of the Ministry of Education. His main research interests include non-traditional machining and surface modification by atmosphere pressure plasma.

Zhu-Ji Jin, born in 1967, is currently a professor and a PhD candidate supervisor of Key Laboratory for Precision and Non-traditional Machining Technology of the Ministry of Education, Dalian University of Technology, China. His main research interests include non-traditional machining and ultraprecision machining technology.

Claire J. Carmalt, born in 1967, is currently a professor, a PhD candidate supervisor and the Head of Department of Chemistry, University College London, UK. Her main research interests include inorganic chemistry, materials chemistry and organometallic chemistry.

Ivan P. Parkin, born in 1972, is currently a professor and a PhD candidate supervisor at Department of Chemistry, University College London, UK. His main research interests include materials chemistry, inorganic chemistry.

#### Competing Interests

The authors declare that they have no competing interests.

**Funding**

Supported by National Natural Science Foundation of China (Grant No. 51605078), Science Fund for Creative Research Groups of NSFC (51621064), and National Basic Research Program of China (973 Program, Grant No. 2015CB057304). EPSRC are thanked for funding equipment.

**Publisher's Note**

Springer Nature remains neutral with regard to jurisdictional claims in published maps and institutional affiliations.

Received: 26 April 2017 Accepted: 8 August 2018

Published online: 20 August 2018

**References**

- [1] R Fürstner, W Barthlott, C Neinhuis, et al. Wetting and self-cleaning properties of artificial superhydrophobic surfaces. *Langmuir*, 2005, 21(3): 956–961.
- [2] Fei Guo, Qiu-Ying Wen, Yu-Bing Peng, et al. Multifunctional hollow superhydrophobic SiO<sub>2</sub> microspheres with robust and self-cleaning and separation of oil/water emulsions properties. *Journal of Colloid and Interface Science*, 2017, 494: 54–63.
- [3] Peng Wang, Dun Zhang, Ri Qiu, et al. Super-hydrophobic metal-complex film fabricated electrochemically on copper as a barrier to corrosive medium. *Corrosion Science*, 2014, 83: 317–326.
- [4] Yan Liu, Jing-Ze Xue, et al. One-step fabrication of biomimetic superhydrophobic surface by electrodeposition on magnesium alloy and its corrosion inhibition. *Journal of Colloid and Interface Science*, 2017, 491: 313–320.
- [5] C Stamatopoulos, J Hemrle, et al. Exceptional anti-icing performance of self-impregnating slippery surfaces. *ACS Applied Materials & Interfaces*, 2017, 9(17): 10233–10242.
- [6] M Callies, D Quere. On water repellency. *Soft Matter*, 2005, 1(1): 55–61.
- [7] R N Wenzel. Surface roughness and contact angle. *Journal of Physical & Colloid Chemistry*, 1949, 9(53): 1466–1467.
- [8] A B D Cassie, S Baxter. Wettability of porous surfaces. *Transactions of the Faraday Society*, 1944, 40: 546–551.
- [9] M Thieme, R Frenzel, S Schmidt, et al. Generation of ultrahydrophobic properties of aluminum—a first step to self-cleaning transparently coated metal surfaces. *Advanced Engineering Materials*, 2001, 3(9): 691–695.
- [10] Xue-Jun Cui, Xiu-Zhou Liu, Liu Fu, et al. Fabrication and corrosion resistance of a hydrophobic micro-arc oxidation coating on AZ31 Mg alloy. *Corrosion Science*, 2015, 90: 402–412.
- [11] Jin-Long Song, Wen-Ji Xu, Xin Liu, et al. Fabrication of superhydrophobic surfaces on Al substrates via a facile chemical deposition process. *Materials Letters*, 2012, 87: 43–46.
- [12] Bao-Jia Li, Ming Zhou, et al. Design and fabrication of super-hydrophobic surfaces on silicon wafers and study of effects to hydrophobicity. *Chinese Journal of Mechanical Engineering*, 2008, 21(4): 18–21.
- [13] Wei Xu, L Rajesh, et al. Evaporation kinetics of sessile water droplets on micropillared superhydrophobic surfaces. *Langmuir*, 2013, 29: 6032–6041.
- [14] Ya-Hua Liu, L Moevius, et al. Pancake bouncing on superhydrophobic surfaces. *Nature Physics*, 2014, 10(7): 515–519.
- [15] L Moevius, Ya-Hua Liu, Zuan-Kai Wang, et al. Pancake bouncing: simulations and theory and experimental verification. *Langmuir*, 2014, 30(43): 13021–13032.
- [16] D Öner, T J Mccarthy. Ultrahydrophobic surfaces. Effects of topography and length scales on wettability. *Langmuir*, 2000, 16: 7777–7782.
- [17] F Schellenberger, N Encinas, et al. How water advances on superhydrophobic surfaces. *Physical Review Letter*, 2016, 116(9): 096101.
- [18] D T Van, D Andrew, et al. Laser textured superhydrophobic surfaces and their applications for homogeneous spot deposition. *Applied Surface Science*, 2016, 365: 153–159.
- [19] Han-Song Li, Guo-Qian Wang, Ning-Song Qu, et al. Through-mask electrochemical machining of a large-area hole array in a serpentine flow channel. *International Journal of Advanced Manufacturing Technology*, 2017, 89(1–4): 933–940.
- [20] Xiao-Lei Chen, Ning-Song Qu, Han-Song Li, et al. Electrochemical micromachining of micro-dimple arrays using a polydimethylsiloxane (PDMS) mask. *Journal of Materials Processing Technology*, 2016, 229: 102–110.
- [21] Dong-Lin Li, Shu-Bao Yang, Yi Wu, et al. Microstructure of electrochemical machining using a mask by dual power supply. *International Journal of Advanced Manufacturing Technology*, 2017, 89(9–12): 3101–3108.
- [22] Qiao-Ling Hao, Ping-Mei Ming. Fabrication of micro-dimple arrays using modified through-mask electrochemical micromachining. *Applied Mechanics and Materials*, 2015, 703: 146–149.
- [23] K Yamamoto, S Ogata. 3-D Thermodynamic Analysis of Superhydrophobic Surfaces. *Journal of Colloid Interface Science*, 2008, 326(2): 471–477.
- [24] N A Patankar. Transition between superhydrophobic states on rough surfaces. *Langmuir*, 2004, 20(17): 7097–7102.
- [25] F Porcheron, P A Monson. Mean-field theory of liquid droplets on roughened solid surfaces: application to super-hydrophobicity. *Langmuir*, 2006, 22(4): 1595–1601.
- [26] C W Extrand. Model for contact angles and hysteresis on rough and ultraphobic surfaces. *Langmuir*, 2002, 18(21): 7991–7999.

Submit your manuscript to a SpringerOpen® journal and benefit from:

- Convenient online submission
- Rigorous peer review
- Open access: articles freely available online
- High visibility within the field
- Retaining the copyright to your article

Submit your next manuscript at ► [springeropen.com](http://springeropen.com)